Metabolic Capabilities of *Escherichia coli*
II. Optimal Growth Patterns

Amit Varma and Bernhard O. Palsson†

*Department of Chemical Engineering, University of Michigan,
Ann Arbor, MI 48109, U.S.A.*

A modeling formalism has been developed recently, based on stoichiometry and linear optimization, that enables determination of the capabilities of metabolic networks. Both single and multiple simultaneous metabolic demands can be studied within this formalism. Here, we use this approach to determine the ability of *Escherichia coli*'s fueling reactions to meet growth demands. "Growth" within this context is defined as a drain of biosynthetic precursors in an appropriate ratio required to produce cellular components. Maximizing biomass yield on glucose in the absence of maintenance requirements, we obtain a yield of 0.588 g DW g^{-1} glucose, which is higher than experimentally reported values. Inclusion of ATP maintenance costs significantly influences the maximal biomass yield. A maintenance cost of 4–6 ATP molecules per glucose consumed gives maximal biomass yields of 0.4–0.45 g DW g^{-1} glucose, which correspond to experimental observations of biomass yields. The corresponding metabolic flux distribution shows a remarkable consistency with experimental observations of pathway utilization, including the fraction of glucose metabolized through the pentose pathway, use of the anaplerotic reactions and redox metabolism. A sensitivity analysis demonstrates a robustness of the optimal biomass yield and pathway utilization to changes in metabolic demands. This result is important considering the diversity of metabolic demands that the cell can experience under different growth and environmental conditions. The optimal biomass yield varies significantly, approximately 20%, over the range of P/O ratios found in energy-transducing membranes. A new metric that is based on shadow prices is formulated to measure the relative importance of the biosynthetic precursors to biomass generation. Interestingly, it identifies the sugar monophosphates as the best utilized biosynthetic precursors for growth in the absence of maintenance energy, although they are needed in relatively small amounts. With maintenance costs, ATP assumes a similar importance. With acetate as the sole substrate we show numerical comparisons of the optimal flux distribution with experimental determinations reported in the literature. We find the optimal solution to be in close agreement with experimentally determined pathway utilizations, the measured metabolic flux levels and biomass yields. Taken together, the results presented here argue for the hypothesis that observed metabolic behavior is consistent with stoichiometric optimality of growth and that regulation of metabolism strives to achieve this stoichiometric optimality.

---

† Author to whom correspondence should be addressed.

1. Introduction

A central and long-standing objective of cellular physiology has been to understand the metabolic capabilities of living cells. In particular, its main function, namely to meet growth requirements, is of central importance. Given the complexity and lesser known metabolic demands in eukaryotic cells, the selection of a prokaryotic cell for study is logical. *Escherichia coli*, in particular, is well characterized in terms of the demands placed on its metabolism (Ingraham *et al.*, 1983; Neidhardt *et al.*, 1987) and it represents an ideal model for such an undertaking. Furthermore, *E. coli* is an organism of significant historical and contemporary industrial importance. Thus, understanding of its metabolic capabilities and fulfilment of growth requirements is correspondingly of broader interest.

Metabolism is comprised of a complex and interwoven set of biochemical reactions and a systemic analysis is needed to delineate its behavior. Even though much experimental data exist on metabolic biochemistry and on the principles of enzyme catalysis and regulation, systemic analysis of metabolism is hampered by the availability of comprehensive kinetic information for a single cell. This situation is found to be true even for *E. coli*.

Fortunately, a new formalism has been developed that does not require detailed enzyme kinetic knowledge that allows us to address the stated question (Fell & Small; 1986; Watson, 1986; Savinell & Palsson, 1992*a*, *b*). This formalism relies solely on the stoichiometry of biochemical pathways, that is well known. In the preceding paper (Varma & Palsson, 1993), we used this approach to determine the ability of *E. coli* to synthesize biosynthetic precursor molecules. We now turn our attention to the question at hand, namely, how does *E. coli* deal with a balanced set of precursor demands that represent growth?

2. Optimal Growth Pattern on Glucose

The growth requirements for *E. coli* can be represented as an overall reaction:

$$\sum_{\text{all } M} d_M \cdot M \overset{V_{gro}}{\rightarrow} \text{biomass} \tag{1}$$

where M represents the biosynthetic precursors and cofactors, and d_M represents the amount in which they are needed per unit of biomass. The weights d_M have been estimated based on cellular composition (Ingraham *et al.*, 1983) and are shown in Fig. 1(a).

Maximal biomass yield can then be determined by computing the optimal solution for maximum V_{gro} for a fixed glucose uptake rate, V_{glc}. Then the maximum biomass yield is computed as

$$Y_{max} = \frac{X}{Glc} = \frac{(V_{gro)max}}{V_{glc}}. \tag{2}$$

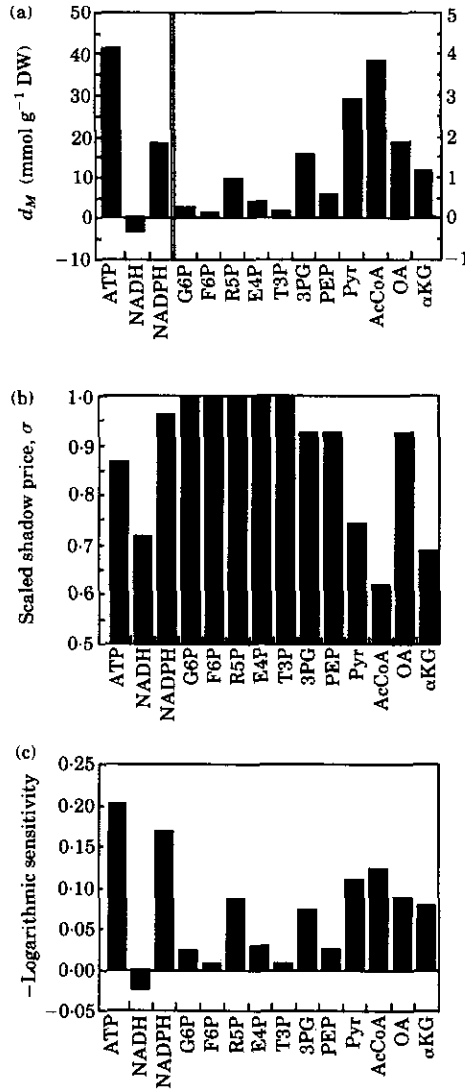The uptake of glucose can either be in mass or molar units. Both units are used

FIG. 1. (a) Metabolic requirements for the production of 1 g of *E. coli* cells, from Ingraham *et al.* (1983). (b) Scaled shadow prices for the maximal biomass yield shown in Fig. 2. (c) Logarithmic sensitivity of maximal biomass yield to the metabolic requirements for growth. The change in sign for NADH reflects a net production of NADH during growth.

below and to convert between them one simply uses the molecular weight of glucose, 180 g mol^{-1} or 0·18 g mmol^{-1}.

Using only the biosynthetic demands, the maximum yield of biomass computed is 0·588 g DW g^{-1} glucose consumed. Under aerobic conditions this yield is higher than typical mass yields of 0·4–0·5 g DW g^{-1} glucose and slightly higher than the maximum experimentally observed values of 0·54 g DW g^{-1} glucose consumed. This

difference is not unexpected since the value of 0·588 d DW g^{-1} glucose is obtained with no maintenance requirements (Schulze & Lipe, 1964). The flux distribution that corresponds to the maximum biomass yield is shown in Fig. 2.

The calculation of the maximum biomass yield leads to two important questions: first, what limits the yield? Second, how sensitive is the optimal solution to changes in fluxes, stoichiometry, biosynthetic demands and the omission of maintenance requirements? We now address these questions.

2.1. WHICH FACTORS CONSTRAIN GROWTH?

Analysis of the shadow prices proved useful when we determined the limiting factors in the production of the biosynthetic precursors (Varma & Palsson, 1993). The shadow prices for the optimal solution presented in Fig. 2 are listed in Table 1. Since all the shadow prices are non-zero, the addition of any one of the precursors will improve the optimal yield. This result is not surprising, since a precursor may not only be directly incorporated into biomass, but also used to generate other biosynthetic precursor molecules. Therefore, each metabolite possibly has multiple values to the cell, such as energy, redox and the potential to make the various carbon skeletons needed.

Thus, the direct use of shadow prices is not useful when multiple simultaneous demands, e.g. V_{gro} in eqn (1), are imposed on the network. A new metric needs to be
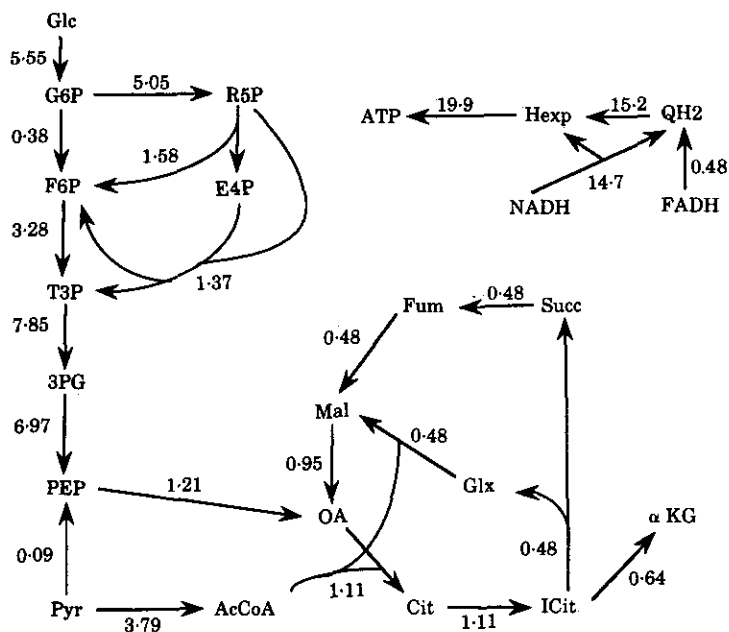

FIG. 2. The optimal flux distribution for aerobic growth on glucose without any maintenance requirements. The maximal biomass production is 0·588 g DW g^{-1} Glc. All fluxes are relative to the input flux of glucose which is 5·55 mmol or 1 g glucose.

TABLE 1

Metabolic demands of precursors and cofactors required for 1 g biomass yield, as well as shadow prices and the identification of growth constraints. The scaled shadow price is shown without considering maintenance as well as for a maintenance requirement of 4 ATP/Glc as described in the text

Metabolite M	d_M (mmol)	Shadow price no maintenance $-\dfrac{\partial X}{\partial M}$	Metabolite yield $-\dfrac{M}{GLC}$	Scaled shadow price σ no maintenance	Scaled shadow price σ 4 ATP/Glc
ATP	41·2570	−0·0049	−18·700	0·863	0·965
NADH	−3·5470	−0·0065	−11·600	0·714	0·921
NADPH	18·2250	−0·0092	−11·000	0·959	0·947
G6P	0·2050	−0·116	−0·908	0·994	0·961
F6P	0·0709	−0·116	−0·908	0·994	0·961
R5P	0·8977	−0·097	−1·080	0·991	0·962
E4P	0·3610	−0·079	−1·330	0·989	0·963
T3P	0·1290	−0·060	−1·740	0·990	0·964
3PG	1·4960	−0·049	−2·000	0·923	0·947
PEP	0·5191	−0·049	−2·000	0·923	0·947
PYR	2·8328	−0·039	−2·000	0·738	0·956
AcCoA	3·7478	−0·033	−2·000	0·615	0·781
OA	1·7867	−0·049	−2·000	0·923	0·816
αKG	1·0789	−0·072	−1·000	0·682	0·829
SuccCoA	—	−0.064	−1·000	0·600	0·741

developed to identify key constraints in such a complex and interconnected network. We will base our development on glucose as the common reference.

Formulation of a metric to assess biomass yield constraints

The factors constraining the biomass yield can be evaluated using the shadow prices of precursors for growth in combination with precursor yields on glucose. Conceptually, the approach taken here is to evaluate whether the cell is producing biosynthetic precursors and cofactors optimally while trying to achieve maximal · biomass yield. If the cell is producing any one of its biosynthetic precursors optimally while maximizing biomass yield, then we assume that this resource is limiting. Under those circumstances, the optimal production of cell mass and the production of this metabolic resource are parallel, or aligned objectives. Conversely, if a metabolic resource is not being optimally produced from glucose, we assume that the cell does not need to optimize the formation of this precursor in order to achieve maximal yield.

The criterion for the identification of yield-limiting factors just outlined is comprised of three different processes. These are:

(i) The optimal incorporation of glucose into biomass:

$$Glc \overset{X/Glc}{\rightarrow} X. \tag{3}$$

The optimal value for (X/Glc) is 0·588 g g^{-1} or 0·106 g mmol^{-1} in the absence of maintenance requirements.

(ii) The optimal yield of a precursor or cofactor from glucose:

$$Glc \overset{M/Glc}{\to} M. \tag{4}$$

These yields (M/Glc) were calculated in the preceding article (Varma & Palsson, 1993) and are listed in the fourth column of Table 1.

(iii) The marginal increase in the biomass yield from glucose if a particular precursor or cofactor were added:

$$M \overset{\partial X/\partial M}{\to} X. \tag{5}$$

The quantity ($\partial X/\partial M$) is the shadow price listed in Table 1.
The biomass yield on glucose through the intermediate M is given by:

$$\left(\frac{M}{Glc}\right) \times \left(\frac{\partial X}{\partial M}\right). \tag{6}$$

In the criterion stated above, this product is to be compared to the biomass yield:

$$\left(\frac{X}{Glc}\right). \tag{7}$$

Since the product of eqn (6) is always less than or equal to the biomass yield of eqn (7), a dimensionless quantity

$$\sigma = \frac{\left(\dfrac{M}{GLC}\right) \times \left(\dfrac{\partial X}{\partial M}\right)}{\left(\dfrac{X}{GLC}\right)} \tag{8}$$

can be defined that assumes numerical values between zero and unity. If σ is unity for a given precursor then we conclude, based on the above line of reasoning, that it is biomass yield limiting. The quantity σ is therefore a shadow price scaled in terms of glucose units and gives a measure of the relative importance of the intermediate for achieving the objective of maximal biomass yield.

After this conceptual development we return to the optimal solution presented in Fig. 2. The numerical values for σ for all the precursors and cofactors are calculated and shown in Fig. 1(b). Interestingly, the sugar monophosphates (G6P, F6P, T3P, R5P, E4P) have σ values closest to unity and are therefore biomass yield-limiting factors under optimal growth on glucose, although they are needed in relatively small amounts. In the case of the cofactors, NADPH is very desirable for biomass production as measured by σ, as is ATP. NADH is not an important constraint as measured by σ, which is as expected because the aerobic network uses NADH only to produce ATP, see Fig. 2.

Another interpretation of the scaled shadow price, σ, is obtained by considering the usefulness of a metabolite to biomass formation. The shadow price of a metabolite represents the marginal utility of that metabolite towards the process of growth. Scaling of the shadow price, as represented by σ, gives the marginal utility of

a metabolite in glucose equivalents. We are thus able to determine the utility of various metabolites on a common basis. For the maximal biomass yield solution, Fig. 2, we find that the sugar monophosphates have the highest utility to the cell.

2.2. HOW SENSITIVE IS THE OPTIMAL SOLUTION?

The optimal solution displayed in Fig. 2 has several noteworthy characteristics. First, the pentose phosphate shunt (PPS) is extensively used. About 91% of the glucose is metabolized through the PPS, which is far greater than experimentally observed values (Wood, 1985). Second, is the use of the glyoxalate shunt as an anaplerotic reaction, which does not normally occur during *E. coli* on glucose. Third, the conversion of Pyr to PEP occurs via the enzyme PEP synthase which is again not normally observed during growth on glucose.

Thus, the optimal solution for maximum biomass yield in Fig. 2 shows some deviations from experimentally determined fluxes. In this section we determine the sensitivity of the maximal biomass yield to various perturbations and thus try to evaluate the factors that determine the differences between experimentally obtained fluxes and the computed optimal solution.

There is a limited number of factors that can influence the optimal solution, given the factors that go into its determination; basically, the metabolic stoichiometry and the metabolic demands. The factors that can affect the optimal solution are:

(i) THE ACTIVE PATHWAYS. Several pathways and reactions that appear in the optimal solution may not be operative in the physiological state considered.

(ii) THE METABOLIC DEMANDS. The biosynthetic requirements used for the generation of 1 g of dry biomass given in Fig. 1(a) are only estimates. These requirements may vary.

(iii) THE P/O RATIO. The stoichiometry of the metabolic network is well known. The one exception is the P/O ratio, since the stoichiometry of energy transducing membranes is not fixed.

(iv) THE MAINTENANCE REQUIREMENT. Living cells have maintenance energy requirements that are not accounted for in the optimal solution presented above.

We wish to characterize the effect of these factors on the maximal biomass yield.

2.2.1. *Constraints on selected pathways*

As pointed out above, the optimal solution has three noteworthy deviations from the expected flux distribution based on experimental data on aerobic growth of *E. coli* on glucose. First, there is a high flux through the pentose pathway. Second, the glyoxylate shunt is used. Third, Pyr is converted to PEP by the enzyme PEP synthase.

The optimal biomass yield was examined with respect to these pathways by restricting the flux through them. Forcing both the glyoxylate shunt and PEP synthase fluxes to zero resulted in a negligible drop in the maximum biomass yield to a value of 0.585 g DW g^{-1} glucose. Thus, the optimal biomass yield is not very sensitive to flux variations through these pathways.
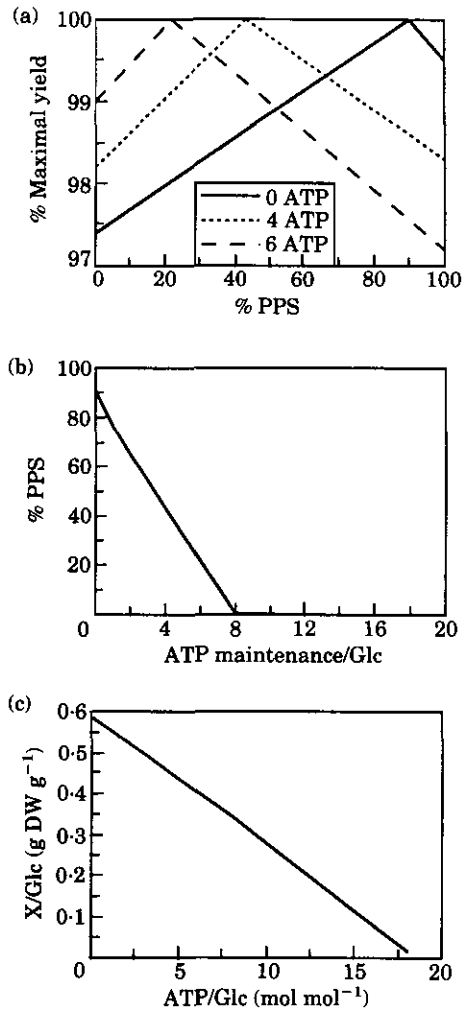
FIG. 3. (a) Yield sensitivity, expressed as a percentage of the maximal biomass yield, plotted as a function of the percentage PPS flux for three different ATP maintenance requirements: 0, 4 and 6 ATP Glc^{-1}. The PPS flux represents the flux through the oxidative branch of the pentose phosphate pathway. (b) Optimal percent PPS flux plotted as a function of ATP maintenance requirements. (c) Variation in maximal biomass yield with changing ATP maintenance requirements.

The maximal biomass yields are relatively insensitive to variations in the flux in the pentose pathway. Shown in Fig. 3(a) is the maximum biomass yield as a function of the pentose pathway flux. Even if the pentose pathway flux is restricted to zero, the maximal biomass yield only drops by 2·5%. Thus, the cell has significant flexibility in determining the metabolic flux distribution around the G6P node without experiencing detrimental effects on the biomass yield. We will discuss later the influence that ATP maintenance energy has on the pentose pathway flux.

2.2.2. *Biosynthetic demands*

The metabolic requirements to produce 1 g of dry cell weight listed in the second column of Table 1 are based on estimates from experimental measurements of cellular composition (Ingraham *et al.*, 1983). The estimates are strain-specific and can also change under different environmental conditions. It is therefore pertinent to calculate the sensitivity of the maximal biomass yield to perturbations in the biosynthetic requirements.

Since the biosynthetic demands vary significantly in their absolute values, we compare the possible errors in their estimates using a relative, or a logarithmic sensitivity, coefficient:

$$\frac{\partial X/X}{\partial d_M/d_M} = \frac{\partial \ln X}{\partial \ln d_M},\tag{9}$$

where d_M is the biosynthetic demand. The logarithmic sensitivity measures the percentage change in the biomass yield in response to a percentage change in the precursor requirement. Logarithmic sensitivity coefficients have become quite popular for the analysis of kinetic models of metabolism following their definition (Savageau, 1969; Kacser & Burns, 1973; Heinrich & Rapoport, 1974).

The relative sensitivity coefficients for the biosynthetic precursors and cofactors are calculated as:

$$\frac{\partial X/X}{\partial d_M/d_M} = \frac{d_M}{X} \times \frac{\partial X}{\partial M} \times \frac{\partial M}{\partial d_M}\tag{10}$$

$$= d_M \times \frac{\partial X}{\partial M}\tag{11}$$

since

$$\frac{\partial M}{\partial d_M} = X.\tag{12}$$

Thus, only the shadow prices and the metabolic requirements are needed to compute the logarithmic sensitivity coefficients. The numerical values for the logarithmic sensitivity coefficients are shown in Fig. 1(c).

Examination of the computed logarithmic sensitivity coefficients leads to important observations. First, the biomass yield is not overly sensitive to changes in biosynthetic need of any one of the precursors or cofactors. The highest values for the logarithmic sensitivity coefficient are 0·2 and 0·17 for ATP and NADPH, respectively. Quantitatively, these values mean that if the need for these cofactors increases by 10%, then the biomass yield will drop 2% and 1·7%, respectively. We will discuss further the ATP maintenance demand below.

Second, changes in the use of biosynthetic precursor molecules do not significantly change the biomass yield. For the bacteria, this feature is highly desirable since biosynthetic demands will always vary from one environmental condition to another. Moderate deviations from the values for d_M listed in Table 1 thus do not have overly detrimental effects on the biomass yield. From an evolutionary and taxonomic standpoint, these results are interesting. This flexibility in meeting metabolic

demands provides the basis for the evolution of a number of different biomass compositions without losing significantly in biomass yield and, thus, without significant loss in competitive advantage. This metabolic network thus can serve the metabolic requirements of many different genomes.

Finally, these results are encouraging for the purpose of redirecting fluxes in bacteria or to "metabolically engineer" them (Bailey, 1991; Stephanopoulos & Vallino, 1991). Moderate diversion of metabolic resources should not lead to engineered strains with vastly inferior growth characteristics. The question of excessive drains is addressed below.

2.2.3. *The P/O ratio*

The P/O ratio is defined as the number of high-energy phosphate bonds formed during the transfer of a pair of electrons to oxygen from NADH via the electron transfer system (ETS). The P/O ratio is determined by two independent factors; the number of protons translocated by the NADH dehydrogenases and the stoichiometry of ATPase.

The enzyme NADH dehydrogenase (ndh) transfers hydrogen from NADH to quinone. Both energy-linked and unlinked activities have been observed (Poole & Haddock, 1974). Use of the non-energy linked activity results in a P/O ratio of 0·667 as compared to a P/O ratio of 1·33 for the energy linked dehydrogenase, assuming an ATPase stoichiometry of $3 H^+/ATP$. Figure 4(a) depicts the maximal biomass yield with either of the NADH dehydrogenases. The use of the non-energy linked NADH dehydrogenase, i.e. reducing the P/O ratio by 50%, results in a significant drop in the biomass yield, to $0·519 g DW g^{-1}$ glucose, a drop of 11·7%.

The energy of the transmembrane proton gradient is converted into high-energy phosphate bonds by the enzyme ATPase. The exact stoichiometry of the conversion is not accurately known. A value of $3 H^+/ATP$ has been used for our analysis, however, non-integral values are possible (Kashket, 1982, 1983; Maloney, 1987). The effect of deviations in the P/O ratio, due to ATPase stoichiometry, on the optimal biomass yield is also shown in Fig. 4(a). The use of $H^+/ATP = 2$ which corresponds to a P/O ratio of 2, i.e. an increase of 50%, results in a biomass yield of 0·625 g dry cells per gram glucose, an increase of 6·3%. On the other hand, a lower P/O ratio of 2/3 (corresponding to $H^+/ATP = 6$), a drop of 50% reduces the biomass yield to 0·514 g biomass per gram glucose, a 12·6% drop. The yield is slightly more sensitive to a P/O ratio change caused by ATPase stoichiometry as compared to ndh.

Thus, we find that within the limits of P/O ratio from 2/3 to 2 ($\pm 50\%$ from our nominal value of 1·33) the maximum biomass yield can vary from 0·514 to $0·625 g DW g^{-1}$ glucose (a 19% range). For the results presented here, the P/O ratio of 1·33 recommended in the literature (Maloney, 1987) has been used. The considerable range of biomass yield argues for the evolution of specialized energy-transducing membranes to carry out terminal oxidation. Higher organisms do, indeed, show specialized structures, e.g. mitochondria and chloroplasts, that are capable of more efficient energy transduction.

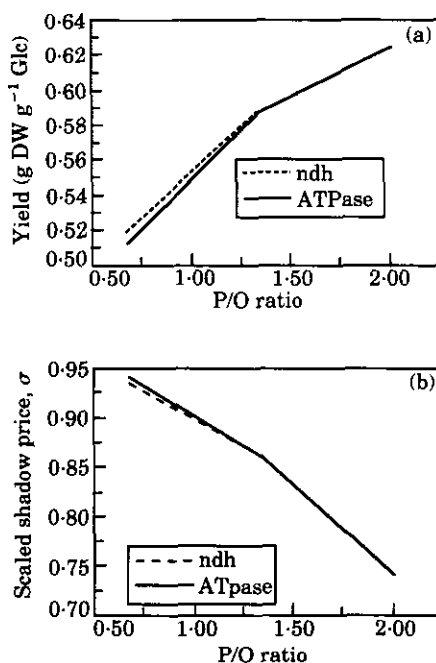Figure 4(b) shows the changes in the scaled shadow price for ATP with changes in

Fig. 4. (a) The optimal biomass yield as a function of the P/O ratio. The two curves represent changes in the P/O ratio due to different stoichiometries of NADH dehydrogenase (ndh) and ATPase. (b) σ value for ATP as a function of the P/O ratio. The P/O ratio is a combination of the reactions catalyzed by the NADH dehydrogenase and cytochromes and ATPase.

the P/O ratio. As expected with a lower P/O ratio, ATP production assumes a greater importance which is reflected in the relative increase in the σ value for ATP from a value of 0·7 at P/O = 0·67. The increases in the σ value indicates the tendency of the maximal biomass solution to move towards the maximal ATP production solution with a reduction in the P/O ratio.

2.2.4. *ATP maintenance requirements*

Cells use energy for metabolic functions other than growth. These functions are many, including cellular motility, maintaining cellular osmolarity, macromolecule turnover and the maintenance of transmembrane gradients. Since it has proven difficult, perhaps impossible, to quantify each one of these functions individually, a phenomenological measure known as the maintenance coefficient (Marr *et al.*, 1963; Pirt, 1965) has gained widespread use. It captures all such functions and can be determined experimentally (Schulze & Lipe, 1964). Most maintenance requirements are of energy and may therefore be termed as ATP maintenance requirements. Maintenance represents a significant draining on metabolic resources at low growth rates.

In the stoichiometric framework, maintenance requirements are best incorporated as a specified number of ATP molecules consumed for other activities than growth
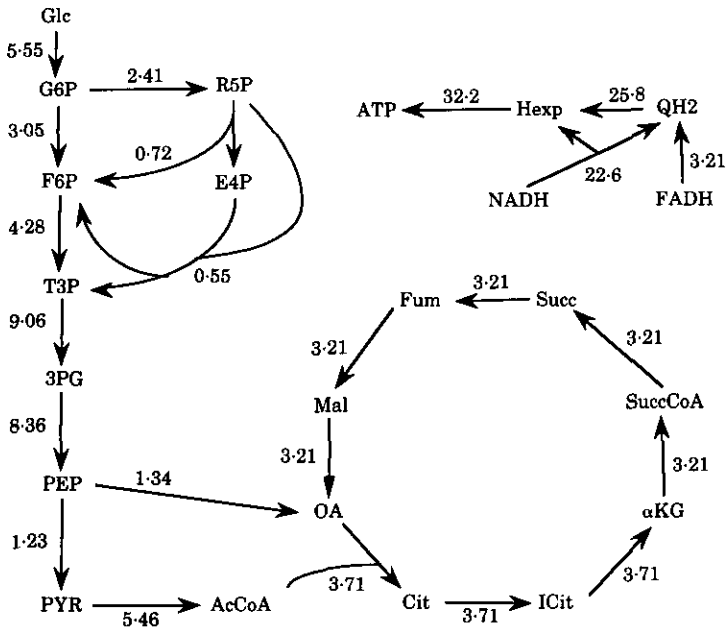
FIG. 5. The optimal flux distribution for aerobic growth on glucose with a maintenance requirement of 4 ATP Glc^{-1}. The maximal biomass production is 0·467 g DW g^{-1} Glc.

per glucose molecule imported into the cell. In this way, the effects of the ATP maintenance needs on the optimal biomass yield are readily calculated. The results of such calculation are shown in Fig. 3(c). The x-axis is given in terms of moles of ATP that are used for maintenance for every mole of glucose consumed. Recall that the ATP shadow price on glucose utilization is 18·7 and, thus, when 18·7 ATP molecules *per* glucose are used for maintenance, the biomass yield drops to zero. The drop in biomass yield with increasing maintenance costs is significant.

Since experimental yields for growth on glucose are in the order of 0·4–0·5 g DW g^{-1} glucose, we show the flux distribution for ATP maintenance requirement of 4 ATP *per* glucose consumed in Fig. 5. The maximal cell yield with this maintenance demand is 0·467 g DW g^{-1} glucose. Note that the fluxes through the glyoxylate shunt and through the PEP synthase have both dropped to zero without imposing any restrictions on these fluxes. Also note that NADPH is produced both by the pentose phosphate pathway as well as from αKG synthesis. Interestingly, there is no contribution of the transhydrogenase reaction to NADPH production, which is consistent with the lack of phenotype for transhydrogenase mutants (Zahl *et al.*, 1978).

Computations of the scaled price, σ, for an ATP maintenance requirement of 4 ATP Glc^{-1} are listed in Table 1. We observe significant changes in the σ values after the inclusion of ATP maintenance requirements. ATP now has the highest value indicating that energy production has acquired an increased importance.

We next examine the PPS flux as a function of the ATP maintenance requirements for maximal biomass yield. The flux through the PPS does show a stoichiometric optimality after considering ATP maintenance requirements. Figure 3(b) plots the computed optimal PPS flux for different maintenance requirements. We find that the optimal PPS flux is very sensitive to the maintenance requirements. In fact, maintenance requirements in the range of 4–6 ATP Glc^{-1} result in optimal PPS fluxes in the physiological range of 20–40% (Wood, 1985). Corresponding to these maintenance requirements, the maximal biomass yield is in the range of 0·5–0·45 g DW g^{-1} glucose which is, again, a physiologically observed range. The maximum biomass yield sensitivity to the PPS flux under ATP maintenance requirements of 4 and 6 ATP glucose^{-1} is shown in Fig. 3(a). The biomass yield varies over a 2·5% range for the entire range of PPS flux.

Thus, the optimal solution obtained with the inclusion of maintenance costs shows pathway utilizations that correspond more closely to experimental observations than the solution without maintenance costs. We therefore observe that microbial metabolism does function in a manner that is consistent with attainment of stoichiometric optimality.

2.3. THE USE OF σ TO INTERPRET THE EFFECTS OF VARIATIONS IN METABOLIC LOADS

The two previous subsections illustrate the development of a metric to rank growth constraining factors and the sensitivity of the optimal solution to variations in stoichiometry and metabolic loads. While the catabolic network displays versatility with respect to attaining high biomass yield in face of stoichiometric variations, changing the metabolic loads does change the flux distribution pattern significantly. The parameter σ can be used to interpret such changes. We will illustrate the use of σ with two examples.

2.3.1. *ATP maintenance requirements*

The variations in the σ value for NADPH and the factors that it is comprised of with changing ATP maintenance requirement are shown in Fig. 6. The computed σ values show a pattern with several discontinuities. The continuous changes in σ are due to continually varying biomass yields and NADPH yields on glucose. On the other hand, the discontinuities in σ arise because of discontinuities in the shadow price for NADPH. Discontinuities in shadow prices are a result of changing a constraining boundary. The optimal use of the metabolic pathways changes resulting in step changes in the shadow price.

Let us now examine a particular discontinuity more closely in order to illustrate the shifting of constraints. The discontinuity chosen is the one occurring between a maintenance demand of 8 and 8·1 ATP per glucose consumed (Fig. 6). The flux distributions for an ATP maintenance demand of 8 and 8·1 are shown in Fig. 7. The discontinuity occurs in σ value due to a surplus production of NADPH that occurs at an ATP maintenance of 8·1. The surplus NADPH is converted into ATP via the electron transfer system. The surplus of NADPH produced results in the drop of its shadow price. In fact, for an ATP maintenance of 8·1 (Fig. 7), the ratio of the shadow
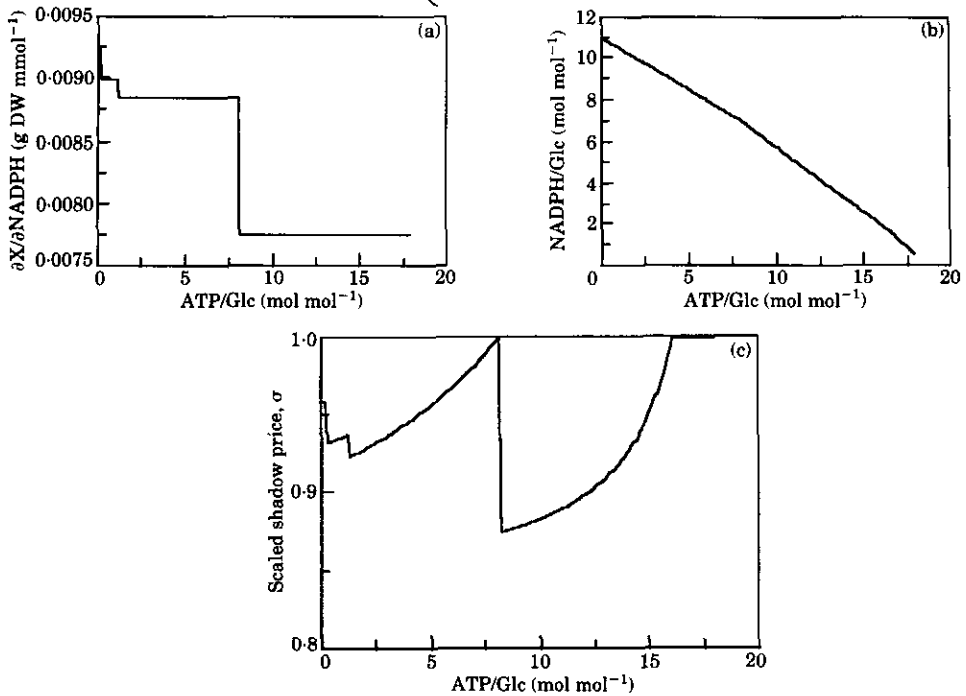
FIG. 6. The derivation of σ values for NADPH from its defining equation shown as a function of the ATP maintenance demand. The maximal biomass yield is displayed in Fig. 4(c). (a) The shadow price of NADPH while optimizing yield on glucose with a varying ATP maintenance demand. (b) The maximal production of NADPH from glucose with the same ATP maintenance demands. (c) σ-values.

prices of NADPH to ATP is 1·33, which is the stoichiometric conversion ratio of NADPH to ATP, while at a maintenance of 8 ATP Glc^{-1}, this ratio of shadow prices is 1·60. Therefore, the value of NADPH is reduced to its ATP equivalence and energy becomes the governing yield constraint. This fact is reflected in the σ value for ATP being changed discontinuously to unity (not shown) while the σ value for NADPH falls to 0·875.

Discontinuities in shadow prices occur due to changes in constraining boundaries (Varma & Palsson, 1993) the consequences of which are a shift in pathway utilization. The increasing demands of ATP for maintenance cause increased utilization of the TCA cycle. Oxidation of ICit to αKG in the TCA cycle results in the concomitant generation of NADPH. At a maintenance requirement of 8·1 ATP Glc^{-1}, a surplus of NADPH is produced that eliminates the need for PPS-produced NADPH. Thus, discontinuity arises and the value of NADPH is reduced to its ATP equivalent as the surplus is funneled down the electron transport system.

2.3.2 Drain of a precursor

Often microbial fermentations are carried out to produce specific products of interest. Useful products usually involve the drain of one or more precursors in order
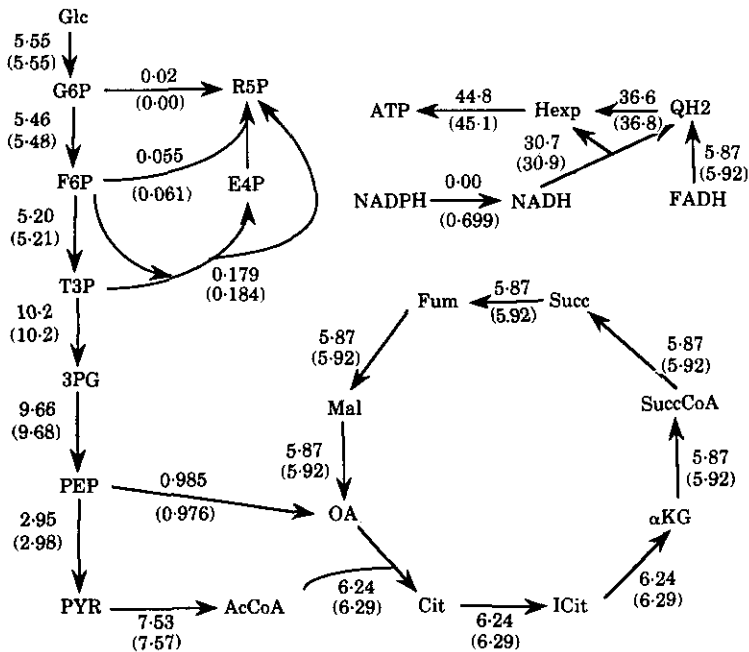
Glc
5·55
(5·55)
G6P $\xrightarrow[\text{(0·00)}]{0·02}$ R5P

ATP $\xleftarrow[\text{(45·1)}]{44·8}$ Hexp $\xleftarrow[\text{(36·8)}]{36·6}$ QH2

5·46
(5·48)
F6P $\xrightarrow[\text{(0·061)}]{0·055}$ E4P

30·7
(30·9)

5·87
(5·92)

0·00
NADPH $\xrightarrow{}$ NADH FADH
(0·699)

5·20
(5·21)
T3P $\xrightarrow[\text{(0·184)}]{0·179}$

10·2
(10·2)

3PG

Fum $\xleftarrow[\text{(5.92)}]{5·87}$ Succ

5·87
(5·92)

5·87
(5·92)

9·66
(9·68)

Mal SuccCoA

5·87
(5·92)

PEP $\xrightarrow[\text{(0·976)}]{0·985}$ OA

2·95
(2·98)

5·87
(5·92)

αKG

6·24
(6·29)

PYR $\xrightarrow[\text{7·53}]{}$ AcCoA $\xrightarrow[\text{(6·29)}]{6·24}$ Cit $\xrightarrow[\text{(6·29)}]{6·24}$ ICit
(7·57)

FIG. 7. Comparison of flux distributions for an ATP maintenance requirement of 8 ATP and 8·1 ATP *per* glucose consumed. Fluxes for 8·1 ATP *per* glucose consumed are shown in parentheses. The ratio of shadow prices for NADPH to ATP is 1·60 for 8 ATP and 1·33 for 8·1 ATP *per* glucose consumed.

to produce the product. We now determine the effects of precursor drain on the biomass yield using the metabolic network formulated.

The intermediate PEP has been chosen as a central metabolite directly or indirectly involved in many biosynthetic fluxes when glucose is used as the carbon source. Figure 8(a) shows changes in the maximum biomass yield with a specified drain of the precursor PEP. As expected, an almost linear decrease in biomass yield is obtained with precursor drain. At a maximal PEP drain of 11·1 mmol g^{-1} glucose the biomass yield drops to zero.

To illustrate the constraints on maximal biomass yield on glucose with an associated PEP drain, the σ values for some metabolites have been plotted in Fig. 8(b). For PEP drains below 8·5 mmol g^{-1} glucose, we note that biosynthetic redox (NADPH) and sugar monophosphates represented by E4P have a high σ value. A PEP drain above 8·5, however, results in surplus ATP and redox being produced as noted by their shadow price dropping to zero. PEP now becomes a governing constraint with all other metabolites showing much lower σ values.

Notable changes occur in the flux distribution at the discontinuity occurring at a PEP drain of 8·5 mmol g^{-1} glucose. At a PEP drain exceeding 8·5 mmol g^{-1}, glucose energy and redox stop being constraints. The flux distribution before the discontinuity may be compared to that after the discontinuity, Fig. 9. At higher PEP drains an excess of energy and redox are produced. Surplus redox is converted to energy
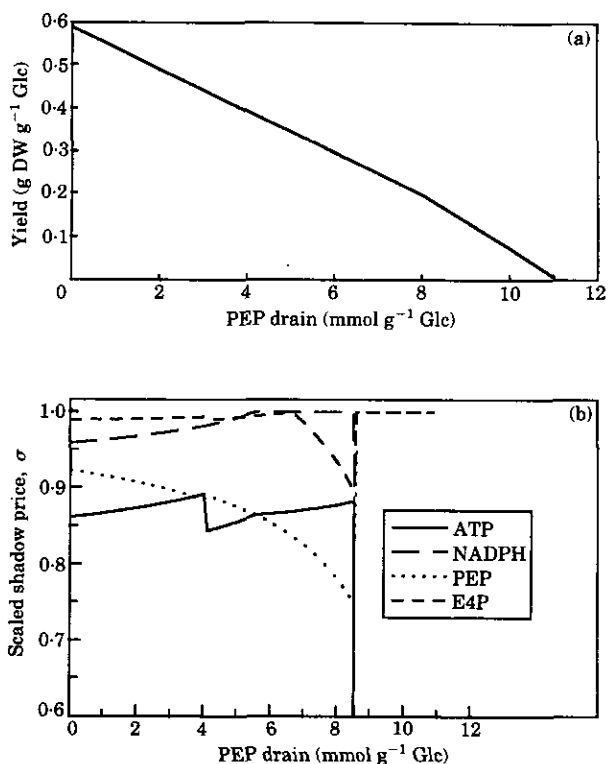
FIG. 8. (a) Maximal biomass yield on a mass basis with a simultaneous drain of the precursor PEP. The precursor drain is defined as mmole per g of glucose. (b) Scaled shadow price, σ, for some intermediates as a function of the drain of the precursor PEP.

through the electron transport system. The net surplus of energy is dissipated in the network by the F6P/FDP futile cycle, as shown in Fig. 9. In the accompanying paper the optimal production of PEP also resulted in the dissipation of surplus ATP through a different futile cycle. Several futile cycles are embedded in the catabolic network, and all can serve to dissipate surplus energy. They all lead to equivalent but different optimal solutions as discussed earlier (Varma & Palsson, 1992). The interpretation of this discontinuity is thus similar to that given above.

3. Growth on Acetate

The flux distribution of *E. coli* growth on acetate is reported in the literature (Walsh & Koshland, 1985). These experimentally determined metabolic fluxes are listed in Table 2. Here, we attempt to compare the experimentally obtained flux distributions to the results computed for maximal biomass yield using the fueling network.

In order to make a suitable comparison, we have to determine the maintenance requirement for growth on acetate. We have therefore computed the maximal
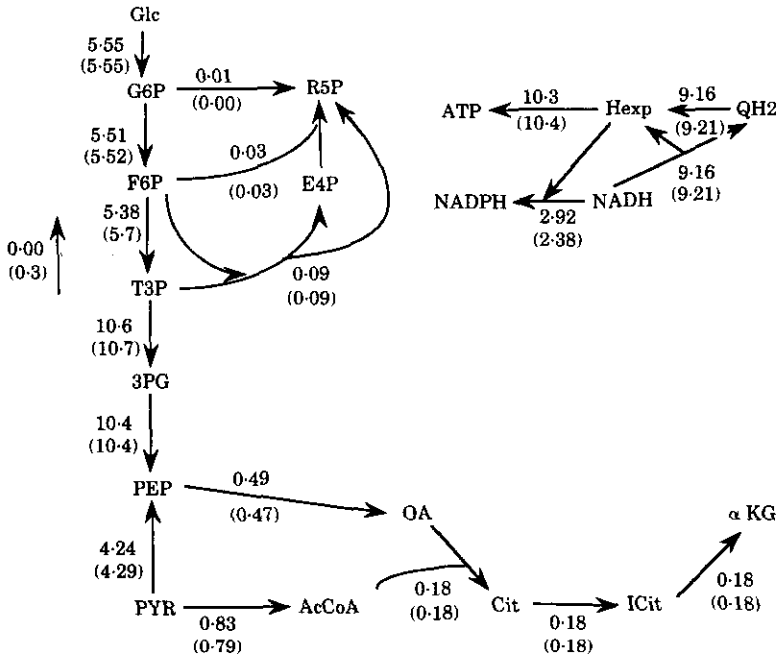
FIG. 9. Comparison of flux distributions for a PEP drain of 8·5 PEP and 8·6 PEP *per* gram of glucose utilized. Fluxes for 8·5 PEP *per* gram glucose consumed are shown in parentheses. For 8·6 PEP the shadow price for energy and redox are zero and surpluses are produced. Surpluses are eliminated through the use of the energy dissipative futile cycle $F6P \rightleftarrows 2 T3P$.

TABLE 2

Flux distribution for growth on acetate for maximum biomass yield compared to experimentally observed values reported in the literature (Walsh & Koshland, 1985). *All fluxes are relative to the same input flux of* 145 *for acetate. The last column shows the flux distribution obtained with the inclusion of an ATP maintenance demand of* 1·5 *ATP per acetate in the metabolic network*

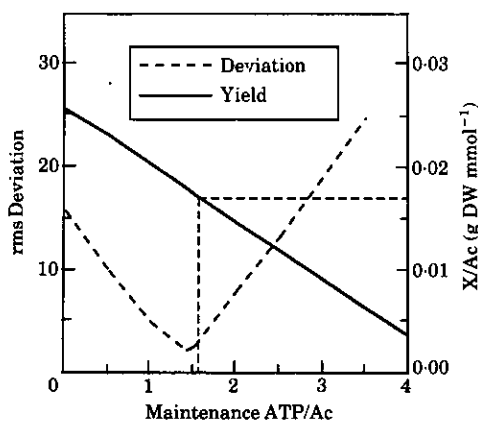|		Optimal fluxes	
Enzyme	Experimental flux	No maintenance	With maintenance
PYRDH	0·0	0·0	0·0
CITSYN	111·0	92·3	109
ISODHP	80·0	53·6	82·7
AKGDH	75·0	49·6	80·0
SUCCDH	106·0	88·3	106
MALDH	127·5	116·0	126
ISOLYS	31·0	38·7	26·4
MALENZ	9·5	10·6	7·2
PEPCK	9·5	17·4	11·9

FIG. 10. Maximal biomass yield on acetate plotted as a function of the ATP maintenance requirements. The root mean square deviation of the experimental flux distribution from the computed maximal biomass yield solution is also shown as a function of the ATP maintenance requirements.

biomass yield as a function of the ATP maintenance requirements, as shown in Fig. 10. The maximum biomass yield on acetate without maintenance is 0.0255 g DW mmol^{-1} acetate. Such a high yield is not experimentally observed because of maintenance demands. Experimentally observed yields are approximately 0.0163 g DW mmol^{-1} acetate (Damoglou & Dawes, 1968). Based on these biomass yields we can estimate a maintenance requirement of 1.5 ATP acetate^{-1}, see Fig. 10. A maintenance of 1.5 ATP acetate^{-1} may appear to be high considering that the maximum ATP generation by the fueling network is 4.67 ATP acetate^{-1}. However, this maintenance includes the additional costs of acetate uptake by the high-energy consuming acetate scavenging pathway (Brown et al., 1977). The maximal yield for a maintenance requirement of 1.5 ATP acetate^{-1} is 0.0175 g DW mol^{-1} acetate.

We have also computed the flux distributions corresponding to the maximal biomass yield under different maintenance requirements. Two such flux distributions, for no maintenance and a maintenance of 1.5 ATP acetate^{-1} are listed in Table 2. We have evaluated the root mean square deviation for the computed fluxes from the above-mentioned experimental fluxes. The results are plotted against the maintenance requirement, see Fig. 10. We note that the minimum deviation between the computed and measured fluxes occurs around 1.5 ATP acetate^{-1}. Remarkably, by defining a physiologically appropriate ATP maintenance requirement we obtain an optimal flux distribution that is similar to the experimentally observed flux distribution.

Interesting questions have arisen with respect to the use of alternate pathways during growth on acetate. It has been suggested that the glyoxalate shunt is the evolutionary predecessor to the complete TCA cycle (Holms, 1986). Restricting the TCA cycle and thus forcing all the flux through the glyoxalate shunt we obtain the maximal biomass yield of 0.014 g DW mmol^{-1} acetate. The 20% drop in biomass yield would then correspond to the evolutionary pressure for the development of the

TCA cycle. Another alternative for energy generation is the use of the pentose phosphate pathway. However, use of the pentose phosphate pathway for energy generation leads to a maximal computed biomass yield of 0.0109 g DW mmol^{-1} acetate. This yield is substantially lower and provides an argument against the use of the pentose phosphate pathway for energy generation. In conclusion, as it does for growth on glucose, *E. coli*'s use of acetate as a substrate follows stoichiometric optimality principles remarkably closely.

4. Conclusions

The influence of metabolic stoichiometry on cellular function and behavior has been studied within the context of flux balancing and linear optimization. The metabolic capabilities and behavior of *E. coli* have been analyzed within this framework and the results compared to experimental data. Remarkably close agreement between computed optimality and a range of different experimental observations is obtained. Taken together, all the results, obtained in this and the preceding study (Varma & Palsson, 1993), support the hypothesis that the metabolic and growth behavior of *E. coli* is consistent with stoichiometric optimality and the underlying regulation strives to attain behavioral patterns that can be described by stoichiometric optimality principles. Finally, the results presented show that analysis through stoichiometric flux balancing can potentially be used both to guide metabolic engineering of bacteria and to provide teleological arguments for evolutionary pressures on metabolic network design and behavior.

REFERENCES

BAILEY, J. E. (1991). Toward a science of metabolic engineering. *Science* **252**, 1668–1675.

BROWN, T. D. K., JONES-MORTIMER, M. C. & KORNBERG, H. L. (1977). The enzymatic interconversion of acetate and acetyl-coenzyme A in *Escherichia coli*. *J. Gen. Microbiol.* **102**, 327–336.

DAMOGLOU, A. P. & DAWES, E. A. (1968). Studies on the lipid content and phosphate requirement of glucose- and acetate-grown *Escherichia coli*. *Biochem. J.* **110**, 775–781.

FELL, D. A. & SMALL, J. A. (1986). Fat synthesis in adipose tissue. An examination of stoichiometric constraints. *Biochem J.* **238**, 781–786.

HEINRICH, R. & RAPOPORT, T. A. (1974). A linear steady state treatment of enzymatic chains. General properties, control and effector strength. *Eur. J. Biochem.* **42**, 89–95.

HOLMS, W. H. (1986). The central metabolic pathways of *Escherichia coli*: relationship between flux and control at a branch point, efficiency of conversion to biomass, and excretion of acetate. *Curr. Top. Cell. Regul.* **28**, 69–105.

INGRAHAM, J. L., MAALØE, O. & NEIDHARDT, F. C. (1983). *Growth of the Bacterial Cell.* Sunderland, MA: Sinauer Associates Inc.

KACSER, H. & BURNS, J. A. (1973). The control of flux. *Symp. Soc. Exp. Biol.* **27**, 65–104.

KASHKET, E. R. (1982). Stoichiometry of the H$^+$-ATPase of growing and resting, aerobic *Escherichia coli*. *Biochemistry* **21**, 5534–5538.

KASHKET, E. R. (1983). Stoichiometry of the H$^+$-ATPase of *Escherichia coli* cells during anaerobic growth. *FEBS Lett.* **154**, 343–346.

MALONEY, P. C. (1987). Coupling to an energized membrane: role of ion-motive gradients in the transduction of metabolic energy. In: Escherichia coli *and* Salmonella typhimurium. *Cellular and Molecular Biology* (Neidhardt, F. C., ed.) pp. 222–243. American Society for Microbiology.

MARR, A. G., NILSON, E. H. & CLARK, D. J. (1963). The maintenance requirement of *Escherichia coli*. *Ann. N.Y. Acad. Sci.* **102**, 536–548.

NEIDHARDT, F. C. (ed.). (1987). Escherichia coli *and* Salmonella typhimurium. *Cellular and Molecular Biology*. American Society for Microbiology.

PIRT, S. J. (1965). The maintenance energy of bacteria in growing cultures. *Proc. R. Soc. B.* **163**, 224–231.

POOLE, R. K. & HADDOCK, B. A. (1974). Energy-linked reduction of nicotinamide-adenine dinucleotide in membranes derived from normal and various respiratory-deficient mutant strains of *Escherichia coli* K12. *Biochem. J.* **144**, 77–85.

SAVAGEAU, M. A. (1969). Biochemical systems analysis. II. The steady state solutions for an n-pool system using a power-law approximation. *J. theor. Biol.* **25**, 370–379.

SAVINELL, J. M. & PALSSON, B. O. (1992a). Network analysis of intermediary metabolism using linear optimization: I. Development of mathematical formalism. *J. theor. Biol.* **154**, 421–454.

SAVINELL, J. M. & PALSSON, B. O. (1992b). Network analysis of intermediary metabolism using linear optimization: II. Interpretation of hybridoma cell metabolism. *J. theor. Biol.* **154**, 455–473.

SCHULZE, K. L. & LIPE, R. S. (1964). Relationship between substrate concentration, growth rate, and respiration rate of *Escherichia coli* in continuous culture. *Arch. Mikrobiol.* **48**, 1–20.

STEPHANOPOULOS, G. & VALLINO, J. J. (1991). Network rigidity and metabolic engineering in metabolite overproduction. *Science* **252**, 1675–1681.

VARMA, A. & PALSSON, B. O. (1993). Metabolic capabilities of *Escherichia coli:* I. Synthesis of biosynthetic precursors and cofactors. *J. theor. Biol.* **165**, 477–502.

WALSH, K. & KOSHLAND, D. R., JR. (1985). Branch point control by the phosphorylation state of isocitrate dehydrogenase. A quantitative examination of fluxes during a regulatory transition. *J. Biol. Chem.* **260**, 8430–8437.

WATSON, M. R. (1986). A discrete model of bacterial metabolism. *Comp. Appl. Biosci.* **2**, 23–27.

WOOD, T. (1985). *The Pentose Phosphate Pathway*. Orlando, FL: Academic Press.

ZAHL, K. J., ROSE, C. & HANSON, R. L. (1978). Isolation and partial characterization of a mutant of *Escherichia coli* lacking pyridine nucleotide transhydrogenase. *Arch. Biochem. Biophys.* **190**, 598–602.